TÜBİTAK

Turkish Journal of Biology

http://journals.tubitak.gov.tr/biology/

Research Article

Turk J Biol
(2013) 37: 507-513
© TÜBİTAK
doi:10.3906/biy-1203-59

# Probing the architecture of testis and morphology of male germinal cells in the mud crab with the atomic force microscopy

**Mahalingam ANBARASU[1,2], Ramangalingam KIRUBAGARAN[1,*], Gopal DHARANI[1], Thanumalaya SUBRAMONIAM[1]**
[1]Marine Biotechnology, National Institute of Ocean Technology, Ministry of Earth Sciences, Government of India, Chennai, India
[2]Central Marine Fisheries Research Institute, Mandapam Regional Centre of CMFRI, Tamil Nadu, India

**Received:** 26.03.2012 • **Accepted:** 23.12.2012 • **Published Online:** 06.09.2013 • **Printed:** 04.10.2013

**Abstract:** The architecture of testicular lobules, morphology of spermatozoa, and spermatophore in the mud crab, *Scylla serrata*, are described for the first time employing atomic force microscopy (AFM). A fast and simple squash preparation protocol was followed using crustacean physiological saline without distorting the natural structure. Observations provided new insight into the arrangement of lobules and morphology of testicular assembly. It consists of a close network of lobules of different sizes in a radial manner on radially branching basal tubules. Budding of new lobules is another distinguishable feature noted in the network of testicular organization. A thin membranous envelope of the lobule with undulating processes offered indirect evidence on the possible storage of sperm cells within the lumen of the lobule. Spermatozoa of *S. serrata* were of different shapes and sizes, and, depending on the maturational status, they displayed changes in the acrosome vesicle with a significant amount of cytoplasm. Vertical constrictions found in the testicular lobules suggest propulsive extrusion of spermatophoric masses into the central lumen. These observations necessitate further study using AFM and involving molecular probes to elucidate the polymorphic nature of male germinal cells, mechanisms of spermatophore formation, and the phylogenetic relationship among crustaceans in general.

**Key words:** Testis, spermatozoa, spermatophore, *Scylla serrata*, AFM

## 1. Introduction

Crustaceans produce a wide variety of reproductive structures that distinguish them from other arthropod groups such as insects, millipedes, and spiders. The majority of male crustaceans produce special sperm packets called spermatophores. Although spermatophores are found in various other invertebrates including other members of arthropods, crustaceans are unique in the way they are used in sperm transmissions to females (1). The male reproductive system of the mud crab, *Scylla serrata*, is composed of testis and vas deferens enclosing various representative constituents, such as spermatogonia, spermatocytes, spermatids, spermatozoa, spermatophores, and seminal fluid. The above constituents have been demonstrated to vary morphologically and biochemically among decapod crustaceans. One of the earliest descriptions available for a decapod sperm cell was from a lithodid crab, *Lithodes maja* (2). Subsequently, some more observations were also made on the pedunculate spermatophores in the vas deferens region of *Lopholithodes mandii* (3). These morphological depictions of testicular assembly through drawings by the authors and similar attempts made by others were slowly replaced due to the emergence of light microscopic advancement in this field, permitting the illustration by photographic images providing a comprehensive knowledge on the morphology, arrangement, and maturation of male germinal cells, and their subsequent packaging into spermatophores.

Ultrastructural visualization of spermatophoric elements was made possible in the 1960s by employing electron microscopys (4–7). Following this, many structural and functional features of crustacean spermatophoric elements were elucidated through scanning electron microscopy (SEM) and transmission electron microscopy (TEM) (8–13). However, there has been concern about the limitations of light microscopy (14) in illustrating the lobular arrangement in toto. Morphology of spermatozoa has been studied comprehensively using electron microscopy (EM), and electron micrographs have been obtained through fixation of sagittal sections. These have revealed several intrinsic features of crustacean spermatozoa. Nevertheless, in this process, spermatozoa are subjected to complete dehydration, which causes them to lose nearly 50% of their volume during observation by EM (15).

* Correspondence: kiruba@niot.res.in

Atomic force microscopy (AFM) has been extensively employed to delineate the surface features of innumerous samples of biological origin in addition to availing topographic data images with nanometer resolution. Spermatozoa have been demonstrated to be better subjects for imaging through AFM because of its rigidity and relatively small size (16). AFM requires simple sample preparation protocols such as usage of physiological saline and air drying of smeared spermatozoa as compared to the use of artificial preservatives and elaborate sample preparation protocols in EM (17). AFM has been successfully used to view the surface topography of sperm heads of numerous mammals (15–21). Despite the vast development achieved technologically in the process of visualization and image capture, and intensive investigation in the field of molecular reproduction of crustaceans in the past century, some of the intrinsic structures, such as architectural arrangement of testicular lobules, remain elusive and are only hypothetical. In the present work, an attempt was made to elucidate the network of lobular organization of the testis, morphology of spermatozoa, and formation of spermatophore in the testis of the mud crab *S. serrata,* using AFM.

## 2. Materials and methods

### 2.1. Animal maintenance

The adult male mud crabs *S. serrata* were collected from the Kovalam coast in Chennai by fishermen. The collected animals were brought to the Seafront Laboratory at Neelankarai and acclimatized to laboratory conditions for 10 days after they were subjected to stringent quarantine treatment. During the period of acclimatization, the animals were maintained in filtered seawater with appropriate water quality parameters, such as salinity (35 ppt), pH (8.1), dissolved oxygen (4.6 mg $L^{-1}$), ambient temperature (25–27 °C), ammonia (~1.2 mg $L^{-1}$), nitrate (~1.4 mg $L^{-1}$), and nitrite (~ 1.4 mg $L^{-1}$). The crabs were fed mussels and clams ad libitum throughout the period of maintenance in the laboratory.

### 2.2. Tissue processing

The crabs were killed by chilling in a freezer (–20 °C) and the testis was dissected out immediately. The testicular mass was macerated with the help of fine scissors and the suspension containing cellular and tissue fragments was diluted with an appropriate amount of physiological saline solution (22) containing the following composition (mM): NaCl 557, KCl 14, $CaCl_2$ 25, $MgCl_2$ 21, $Na_2SO_4$ 4.5, and Tris 5, and the pH was adjusted to 7.4. The above suspension was dropped onto ethanol cleaned glass cover slips using a wide pore tip fitted micropipette and spread uniformly with the help of another glass cover slip. The sample was allowed to adhere to the surface by air drying briefly. Adhered samples were rinsed briefly with nanopure water and then air dried. Care was taken not to damage the sample applied surface on the cover glass. The samples were then mounted to the AFM stub (18 mm Ø × 2 mm thickness), keeping the sample applied area facing upward by using a small piece of double-sided adhesive tape and loaded into the AFM with tweezers.

### 2.3. Image processing

Topographical images of the samples were obtained in a contact mode using an atomic force microscope (Shimadzu Corporation, Kyoto, Japan; SPM-9500) equipped with a phase imaging system and data processing unit. The system was allowed to collect topographical information of applied samples with repetitive scanning under a sharp contact probe. The probe was attached to a cantilever that deflected the direction of the Z-axis as the probe was drawn over the surface of the sample. As the scanning probe was deflected by changes in the sample thickness, the AFM adjusted the position of the sample to maintain a minimal set point deflection of the cantilever. These adjustments were recorded by the computer, and used to generate a high resolution topographical map of the samples kept under observation.

The silicon nitride probes coated with gold used in this study had a pyramidal tip with 6-µm square base and an opening angle of 70°. This tip was attached to a 200-µm long triangular cantilever with a spring constant of 0.15 N/m and resonance frequency of 24 kHz. Before the samples were observed, the piezoelectric scanner was calibrated using standard gratings as per the guidelines of the manufacturer mentioned above. Deviations between the actual and AFM measured distances on the grating indicated that the maximum calibration error in calculated volume measurements could be < 5%. This was reduced significantly (to <3%) by keeping the AFM scanner offset less than 15 µm from the neutral position. Repetitive scanning of a single area took approximately 5–10 min, depending on the objects. Scanned images stored in the computer integrated with the AFM were analyzed for fine surface topography of testicular lobules, and morphology of male germinal cells and spermatophore using AFM software. AFM provided detailed information about the size and shape of various male germinal cells and spermatophore, in addition to lobular arrangement of the testis in this study. Images of 256 × 256 pixels were collected at ambient humidity and the temperature was recorded at an appropriate line frequency.

## 3. Results and discussion

In the present investigation, AFM observation of male reproductive assembly of *S. serrata* presented newer details on the arrangement of testicular lobules, structure of male

germinal cells in different stages, and spermatophore formation. The testicular lobules of *S. serrata* are formed in a radial manner all along branching basal tubules as shown in Figure 1. Several such radially branching tubes join together to form a common collecting duct. The centrally located tubules serve as a common collecting duct for many basal tubules. Several such centrally formed collecting ducts may join together in a convoluted manner and run into the proximal vas deferens, which in turn forms into a mid and distal vas deferens for storage and ejaculation of spermatophoric substances. A closely arranged network of lobules of different sizes was also noted (Figure 1). Generally, in decapod brachyuran crustaceans, the process of spermatogenesis is completed in testis and the spermatozoa travel towards vas deferens before incorporating into spermatophores and are stored with the surrounding fluid medium of seminal plasma (23). Each lobule originates from a basal tubule and is found intercalated with the counterpart shooting from the opposite direction. The distal part of the lobule becomes distended and forms a bulbular structure. The continuous formation of testicular lobules all along the basal tubules also indicates the possibility to meet the requirements during the accelerated spermatogenic activity as a part of testicular maturational processes. Numerous budding lobules were also seen throughout the length of each basal tubule (Figure 2), providing ample scope for further enlargement of the budding lobule, which ultimately

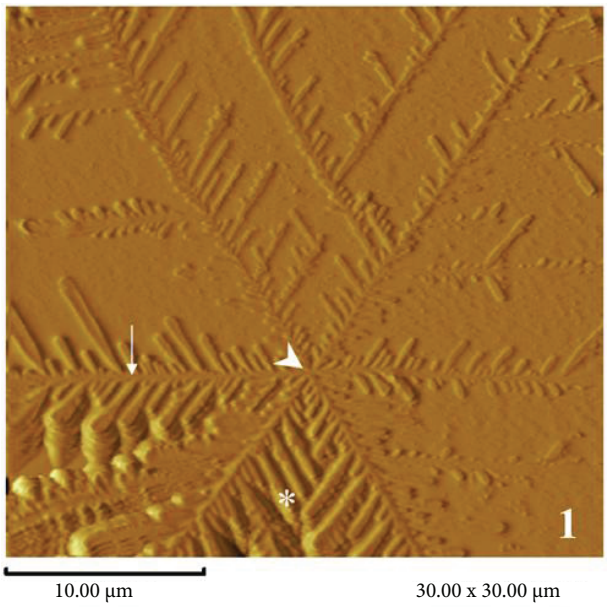


**Figure 1.** Shows the arrangement of testicular lobules with radial branching. Arrow and arrowhead indicate a lateral basal tubule and a central collecting duct, respectively. * indicates a typical lobule formation.

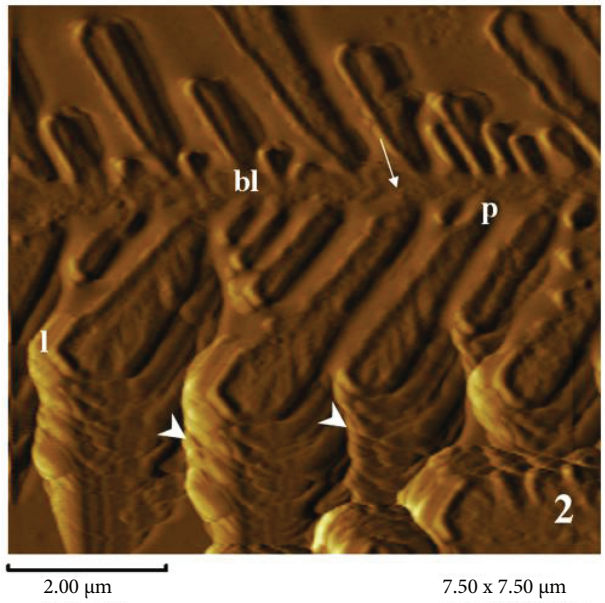


**Figure 2.** Shows the testicular lobule filled with sperm. Arrow heads and arrows show the lemellar nature of the lobule and a basal tubule. l: lobule; bl: budding lobule; p: pedicel.

stores a large volume and a variety of male germinal cells, such as spermatogonia, spermatocytes, spermatids, and spermatozoa in addition to seminal plasma in the lumen. Each lobule was noted along with an indistinguishable pedicel region at the bottom before joining to the basal tubule. The pedicel was considerably broader in this species. At the base of some developing lobules, accessory lobules were also noted, although not uniformly in all cases (Figure 3). An enlarged view of the lobules shows some sort of undulating processes, indicating indirectly the possibility for the presence of several male germinal cells within the lumen of the lobule.

This is the first report providing a clear photographic illustration on the architecture of lobules and connecting tubules in the testicular assembly to a greater extent using AFM. The AFM approach employed in this study could help us to overcome the limitations faced on the illustration of these intrinsic structures through light and electron microscopic attempts made by others so far (14,15). Leaf-like branching lobules shooting from the radially dividing basal tubes further suggest the feasibility of the formation and maturation of sperm cells within the lumen of testicular lobes. The thin lobular membrane enclosing the lumen seems to be elastic and it may have the provision for further enlargement during gonadal maturation. These lobules are of different widths and lengths, implying different phases of sperm maturation occurring differentially in each lumen of the testicular lobules. It denotes progression of sperm cell maturation as occurring in different testicular

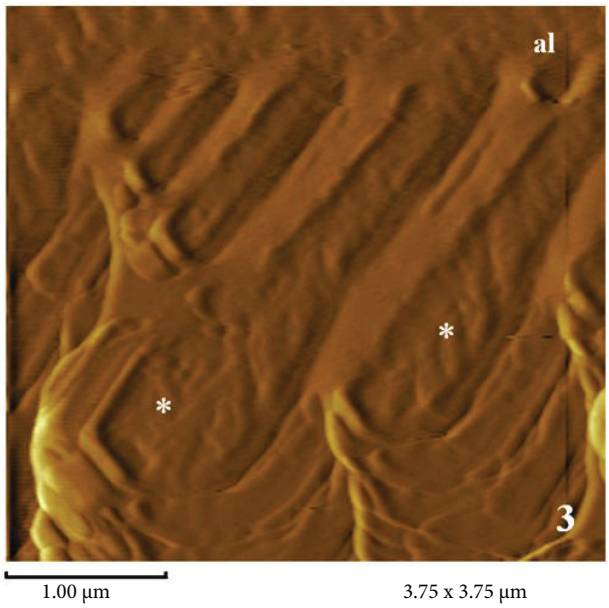


**Figure 3.** Enlarged view of a part from Figure 2. *signifies the possible development of male germinal cells inside. al: accessory lobule.

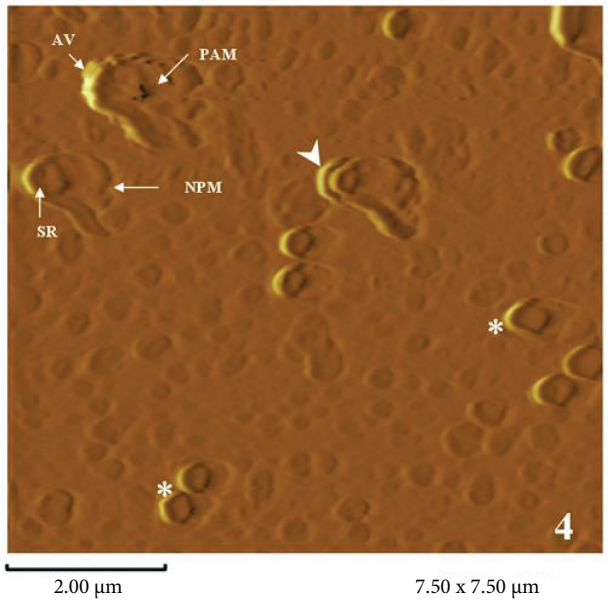


**Figure 4.** Shows the polymorphic nature of male germinal cells at different stages. Arrowhead and *denotes a homogenous outer region and a granular inner region, respectively. AV: acrosome vesicle, NPM: nucleo-plasma envelope; PAM: periacrosomal material; SR: subacrosomal region.

lobules. Interestingly, in *S. serrata* and *Charybdis natator*, testosterone controls spermatophoric activity and hence the formation of testicular lobules could be under its control (24,25). A closely arranged network of lobules intercalating with their counterparts shooting from the adjacent basal tubules was a common phenomenon noted during this investigation. At the base of the lobules, some budding lobules were uniformly distributed close to the pedicel region, although the pedicel was very broad and distinct in this species. The variation in the size of the lobes is very much anticipated even within an individual, depending on the stage of maturation. Nevertheless, the significance of accessory lobes at the base of developed lobules is unknown at present. No other studies conducted earlier could provide such a clear view of the architectural arrangement of testicular assembly.

Male germinal cells of *S. serrata* were of different shapes and sizes, and distributed uniformly in all observed areas as shown in Figure 4. Depending on the stage of maturation, the germinal male cells displayed the shape of the acrosome vesicle, which were seen surrounded by a significant amount of cytoplasm, from spherical to ovoid. The concentric zone of the acrosomal vesicle was also one of the important characteristic features noted in the spermatozoa of *S. serrata.* A conspicuous nucleo-plasma envelope and accumulation of periacrosomal material were the other noticeable structures in the fully matured spermatozoa. As observed in the present study, the squash preparation of testicular lobes showed many different sized and shaped sperm cells, revealing a polymorphic nature of male germinal cells with distinct uniqueness, as reported in other crustaceans (25–28). Similar to the observations made in the current study, a complex acrosome vesicle zone concentrically capped by an electron-dense operculum and penetrating posteriorly by a perforatorial chamber was also noted through transmission electron microscopy in the hermit crab, *Loxopagurus loxochelis* (29). This study further reveals the formation of spermatophore assembly within the lumen of the seminiferous tubules of *S. serrata* (Figure 5). In the matured testicular lobules, there were certain constrictive areas suggesting propulsive ejection of seminal substances into the basal tubules. Formed spermatophoric packets were noted sporadically during the examination using AFM with varying dimensions and shapes, and they were also longitudinally multilayered in nature.

An enlarged view of the lobule shows some sort of undulating processes suggesting indirectly the presence of spermatozoa within the lumen (Figure 3). In a study conducted in the male Jonah crab, *Cancer borealis* (26), it was documented that the spermatogonia developed from the germinal layer of testes and gave rise to spermatocysts and spermatids filling the lumen of the tube with the formation of spermatozoa occurring at the periphery of the tubes. The formation of spermatophoric walls was also reported by the presence of incomplete ring-shaped spermatophoric walls within which numerous enclosed spermatozoa were found (Figure 5). However, they were

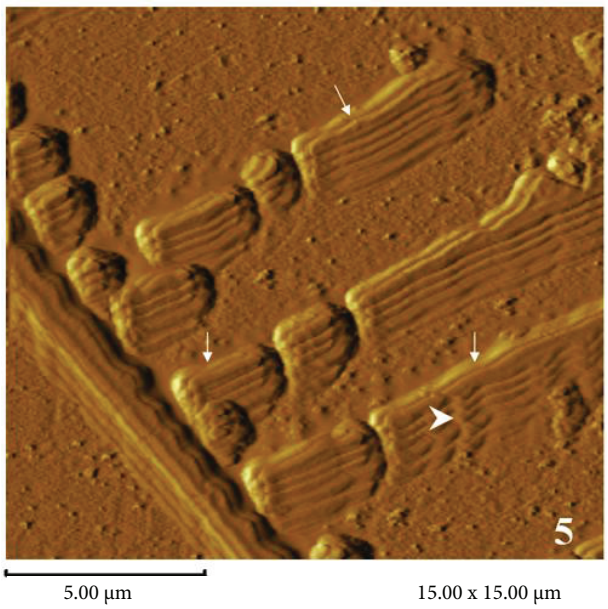


**Figure 5.** Shows sperms stored spermatophoric packets (arrows) of different dimensions; arrowhead points out the appearance of a new vertical constrictive process for formation of spermatophore.

not able to differentiate the vas deferens into different regions based on gross anatomy (25). It was also observed that the number of free spermatozoa increased towards the distal region of the vas deferens. The earliest observations employing light microscopys were made on the hermit crab spermatophore several times in the past (3,30–38). Light microscopic approaches on spermatophore morphology provided further information on the presence of a single layer encompassing the sperm mass in species such as *Carcinus maenas* (39), *Callinectes sapidus* (40), and *Portunus sanquinolentus* (41). In contrast, absence of such an envelope over a spermatophoric mass was also reported in the case of the Hawaiian crab, *Ranina ranina* (42). A double-layered spermatophore has been described in the studies conducted on the mud crab, *S. serrata* (43), and the golden crab, *Geryon fenneri* (23). Notwithstanding the report that only one sperm is contained in each spermatophore in the Oxyrhynchan, *Macrocoeloma trispinosum* (44), a definite variation in the number of spermatozoa distributed has also been noted in the spermatophores of the mud crab, *S. serrata* (45).

In the present observation, the spermatozoa of *S. serrata* were of different shapes and sizes and distributed uniformly in all observed areas (Figures 1–5). Although the term *spermatophore* has been variably used by different authors, it has been restricted as a terminal structure emitted from the male ejaculatory duct (46). However, they have been demonstrated to be structurally complex externally. The spermatophoric packets of variable dimensions were also noted sporadically during the examination using AFM in the present investigation (Figure 5). The presence of such sperm packets, each containing 10–20 sperm cells, was also reported in the middle part of vas deferens (47). The spermatophoric packets observed in *S. serrata* were also longitudinally multilayered in nature. A line of lateral division was also witnessed in another study separating the ampulla into 2 halves (13). These suture lines were reported as the point of weakness where the ampulla breaks to release the spermatozoa prior to fertilization. However, no lateral ridge in the spermatophore was observed in the king crab, *L. maja*, although the spermatophore wall was found to be bilayered (48). In addition, the spermatophoric packets were also observed uniformly, which could be possible due to the emergence of several vertical constrictive processes to cleave them into smaller units.

Nevertheless, to the best of our knowledge, this is the first study carried out on the morphology of spermatozoa and spermatophore of a crustacean model employing AFM. AFM has emerged as the only technique capable of real-time imaging of the surface of a living cell, including sperm cells, at nano-resolution (49). It does not distort sperm morphology as the conventional microscopic techniques do. Recently, a new technique developed based on AFM provides scope to image and to quantify the strength of specific receptor sites on the membrane of living cells (50). Stringent maintenance of sperm morphology is the universal prerequisite for successful fertilization related events. Abnormal germinal development leads to infertility. Sperm morphology is considered as one of the primary prognostic parameters including humans (51). Therefore, the current approach opens up new avenue in order to detect several vital receptors and key molecules present at the membrane surface of the spermatozoa of commercially important crustaceans, by binding the antibodies with an AFM tip. In addition, it may also serve as a prognostic tool for identifying the status of spermatozoa of economically important crustaceans for aquaculture practices. Meanwhile, it has been pointed out that studies pertaining to mating behavior, timing of mating during the moult cycle, sperm transfer mechanisms, male sexual tube morphology and microstructure, and ultrastructure of egg, spermatophore and sperm cell in crustaceans are imminent and would be fruitful. Application of AFM in this regard would certainly provide vast knowledge further required in this field.

**Acknowledgment**
This research was funded by a grant from the Ministry of Earth Sciences, Government of India.

## References


1. Subramoniam T. Spermatophore and sperm transfer in marine crustaceans. Adv Mar Biol 29: 129–214, 1993.
2. Retzius G. Die Spermien der Crustaceen. Biol Untersuch 14: 1–54, 1909.
3. Fasten N. Male reproductive organs of decapoda, with special reference to Puget Sound forms. Puget Sound Mar Stat Publ 1: 285–307, 1917.
4. Dhillon B. Sperm nucleus of *Clibanarius longitarsus*. Experientia 20: 505–506, 1964.
5. Pochon-Masson J. L'ultrastrucure des épines du spermatozoïde chez les Décapodes (Macroures, Anomoures, Brachyoures). Comptes Rendus Hebdomadaire des Séances de l'Academie des Sciences, Paris 260: 3762–3764, 1965.
6. Chevaillier P. Structure et constitution cytochimique de la capsule du spermatozoïde des Crustacés Décapodes. Comptes Rendus Hebdomadaire des Séances de l'Academie des Sciences, Paris 262: 1546–1549, 1966.
7. Chevaillier P. Nouvelles observations sur la structure des fibres intra-nucléaires du spermatozoïde du Pagure Eupagurus bernhardus L. (Crustacé, Décapode). J de Microscopie 6: 853–856, 1967.
8. Tudge CC. Spermatophore diversity within and among the hermit crab families, Coenobitidae, Diogenidae, and Paguridae (Paguroidea, Anomura, Decapoda). Biol Bull 181: 238–247, 1991.
9. Tudge CC. Ultrastructure and phylogeny of anomuran crab spermatozoa, PhD, Department of Zoology, The University of Queensland, Australia; 1995.
10. Tudge CC. Spermatophore morphology and spermatozoal ultrastructure of the recently described hermit crab *Strigopagurus boreonotus* Forest, 1995 (Decapoda, Anomura, Diogenidae). Bull Mus Nation His Nat Paris 18: 547–555; 1996.
11. Tudge CC. Phylogeny of Anomura (Decapoda, Crustacea): Spermatozoa and spermatophore morphological evidence. Contrib Zool 67: 125–141; 1997.
12. Tudge CC. Spermatophore morphology in the hermit crab families Paguridae and Parapaguridae (Paguroidea, Anomura, Decapoda). Invetebr Reprod Dev 35: 203–214; 1999.
13. Tudge CC. Ultrastructure of the spermatophore lateral ridge in hermit crabs (Decapoda, Anomura, Paguroidea). Crustaceana 72: 77–84; 1999.
14. Tudge CC. Endemic and enigmatic: the reproductive biology of Aegla (Crustacea: Anomura: Aeglidae) with observations on sperm structure. Memoir Mus Victoria 60: 63–70; 2003.
15. Allen MJ, Lee JD 4th, Lee C et al. Extent of sperm chromatin hydration determined by atomic force microscopy. Mol Reprod Dev 45: 87–92; 1996.
16. Lee JD, Allen MJ, Balhorn R. Atomic force microscopy analysis of chromatin volumes in human sperm with head-shape abnormalities. Biol Reprod 56: 42–49; 1997.
17. Allen MJ, Bradbury EM, Balhorn R. The natural subcellular surface structure of the bovine sperm cell. J Struct Biol 114: 197–208; 1995.
18. Saeki K, Sumitomo N, Nagata Y et al. Fine surface structure of bovine acrosome: intact and reacted spermatozoa observed by atomic force microscopy. J Reprod Develop 51: 293–298; 2005.
19. Allen MJ, Bradbury EM, Balhorn R. The chromatin structure of well-spread demembranated human sperm nuclei revealed by atomic force microscopy. Scanning Microscopy 10: 989–996; 1996.
20. Ellis DJ, Shadan S, James PS et al. Post-testicular development of a novel membrane substructure within the equatorial segment of ram, bull, boar, and goat spermatozoa as viewed by atomic force microscopy. J Struct Biol 138: 187–198; 2002.
21. Soon LL, Bottema C, Breed WG. Atomic force microscopy and cytochemistry of chromatin from marsupial spermatozoa with special reference to *Sminthopis crassicaudata*. Mol Reprod Dev 48: 367–374; 1997.
22. Yamagishi H, Ebara A. Spontaneous activity and pacemaker property of neurones in the cardiac ganglion of an isopod crustacean, *Ligia exotica.* Comp Biochem Physiol 81A: 55–62; 1985.
23. Hinsch GW. Ultrastructure of sperm and spermatophores of the golden crab *Geryon fenneri* and a closely related species, the red crab *G. quinqendens*, from the eastern Gulf of Mexico. J Crustacean Biol 8: 340–345; 1988.
24. Sheeba JR, Sasikala SL, Kirubagaran R et al. Role of serotonin on testicular maturation in the male mud crab, *Scylla serrata* (Forskal, 1775). Proceedings of XXII Symposium on Reproductive Biology and Comparative Endocrinology held at University of Madras, Chennai, India; 2004.
25. Helen SB, Jamila PE, Kirubagaran R. Variations in vertebrate-type steroids during testicular maturation in the marine crab, *Charybdis natator* (Herbst). J Mar Biol Assoc India 48: 241–244; 2006.
26. Moriyasu M, Benhalima K, Duggan D et al. Reproductive biology of male Jonah crab, *Cancer borealis* Stimpson, 1859 (Decapoda, Cancridae) on the Scotian Shelf, Northwestern Atlantic. Crustaceana 75: 891–913; 2002.
27. Jamieson BGM, Tudge CC. Crustacea- Decapoda. In: Jamieson BGM, Wiley CJ eds. Progress in Male Gamete Ultrastructure and Phylogeny; 2000: Vol. 9 Part C, pp. 1–95.
28. Tudge CC, Scheltinga DM. Spermatozoa morphology of the freshwater anomuran Aegla longirostri Bond-Buckup & Buckup, 1994 (Crustacea: Decapoda: Aeglidae) from South America. Proc Biol Soc of Washington 115: 118–128, 2002.
29. Scelzo MA, Medina A, Tudge CC. Spermatozoal ultrastructure of the hermit crab *Loxopagurus loxochelis* (Moreira, 1901) (Decapoda: Anomura: Diogenidae) from the southwestern Atlantic. In: Asakura A. ed. Biology of Anomura II. Crustacean Research; 2006: Vol. 6, pp. 1-11.

30. Mouchet S. Mode de formation des spermatophores chez quelques Pagures. Comptes Rendus Hebdomadaire des Séances de l'Academie des Sciences, Paris 190: 691–693; 1930.

31. Mouchet S. Spermatophores des Crustacés Décapodes Anomoures et Brachyoures et castration parasitare chez quelques Pagures. Annales de la Station Océanographique de salammbô 6: 1–203; 1931.

32. Hamon M. La constitution chimique des de Custaceés supérieurs du groupe des Pagurides. Comptes Rendus Hebdomadaire des Séances de l'Academie des Sciences, Paris 204: 1504–1506; 1937.

33. Hamon M. Les mechanisms produisant la dehiscence des spermatophores *d'Eupagurus prideauxi* Leach. Comptes Rendus Hebdomadaire des Séances de la Société de Biologie 130: 1312–135; 1939.

34. Hamon M. Researches sur les spermatophores. Théses présentées a las faculté Sciences de l' Université d'Alger, Maĺson-Carrée, Alger 1–185; 1942.

35. Mathews DC. The development of the pedunculate spermatophore of a hermit crab, *Dardanus asper* (DeHann). Pacific Sci 7: 255–266; 1953.

36. Mathews DC. The origin of the spermatophoric mass of the sand crab, *Hippa pacifica.* Quart J Microsc Sci 97: 257–268; 1956.

37. Mathews DC. Further evidences anomuran non-pedunculate spermatophores. Pacific Sci 11: 380–385; 1957.

38. Greenwood JG. The male reproductive system and spermatophore formation in *Pagurus novae-zealandiae* (Dana) (Anomura: Paguridae). J Nat Hist 6: 561–574; 1972.

39. Spalding JF. The nature and formation of spermatophore and sperm plug in *Carcinus maenas.* Q J Microsc Sci 83: 399–422; 1942.

40. Cronin LE. Anatomy and histology of the male reproductive system of *Callinectes sapidus*. Rathbun. J Morphol 81: 209–239; 1947.

41. Ryan EP. Structure and function of the reproductive system of the crab *Portunus sanguinolentus* (Herbst) (Brachyura: Portunidae). Mar Biol Assoc India (Sympo. Ser.) 2: 506; 1967.

42. Ryan EP. Spermatogenesis and male reproductive system in the Hawaiian crab *Ranina ranina* (L.). In: Engeles W. ed. Advances in Invertebrate Reproduction. Elsevier; 1984: p. 629.

43. Uma K, Subramoniam T. Histochemical characteristics of spermatophore layers of *Scylla serrata* (Forskal) (Decapoda: Portunidae). Int J Inver Repr 1: 31–41; 1979.

44. Hinsch GW. Sperm structure of *Oxyrhyncha.* Cana J Zoolog 51: 421–426; 1973.

45. Jeyalectumie C, Subramoniam T. Biochemistry of seminal secretions of the crab *Scylla serrata* with reference to sperm metabolism and storage in the female. Mol Reprod Develop 30: 44–55; 1991.

46. Bauer RT. Sperm transfer and storage structures in penaeoid shrimps: A functional and phylogentic perspective. In: Bauer RT, Martin W. eds. Crustacean Sexual Biology. New York Columbia University Press; 1991: pp. 183–207.

47. Diesel R. Structure and function of the reproductive system of the spider crab *Inachus phalangium* (Decapoda: Majidae): Observations on sperm transfer, sperm storage and spawning. J Crustacean Biol 9: 266–277; 1989.

48. Tudge CC, Jamieson BGM, Sandberg L et al. Ultrastructure of mature spermatozoon of the king crab *Lithodes maja* (Lithodidae, Anomura, decapoda): Further confirmation of a lithodid–pagurid relationship. Invertebr Biol 117: 57–66; 1998.

49. Kumar S, Chaudhury K, Sen P et al. Atomic force microscopy: a powerful tool for high-resolution imaging of spermatozoa. J Nanobiotechno 3: 9–13; 2005.

50. McElfresh MW, Rudd RE, Balhorn R et al. Probing the properties of cells and cell surfaces with the atomic force microscopy. LDRD Final Report 01-ERI-001 (UCRL-TR-202443); 2004.

51. Franken RD. The clinical significance of sperm-zona pellucida binding. Front Biosci 3: 247–253; 1998.